ce/papers Proceedings in civil engineering

Ernst & Sohn A Wiley Brand

ORIGINAL ARTICLE

EUROSTRUCT

Ductility of RC Columns confined with FRP Sheets

Eftychia Apostolidi[1] | Efstathia Liakopoulou[2] | Stephanos Dritsos[2] | Danièle Waldmann-Diederich[1]

Correspondence

Dr. Eftychia Apostolidi
Technical University of Darmstadt
Institute for Solid Structures
Franziska-Braun-Straße 3
64287 Darmstadt
Email: apostolidi@massivbau.tu-darmstadt.de

[1] Technical University of Darmstadt, Darmstadt, Germany
[2] University of Patras, Patras, Greece

Abstract

Many existing structures show insufficient seismic capacity, with the lack of members' ductility being a critical factor. Aim is to manage to increase their ductility, through confinement with composite fiber reinforced polymer (FRP) sheets. In the present paper, available analytical procedures of Eurocode 8-Part 3 (2005) and draft of 2022 and the Greek Code for Structural Interventions (CSI) of 2013 and the revision of 2022 are examined, compared together with an analytical model proposed in the literature. Analytical results of the above procedures are also compared both with available experimental data and with each other and the degree of their reliability is evaluated. The current EC8-3 (2005), although in many cases converges quite well with the experimental data, unrealistic results are obtained for a large thickness of the confined material. This seems to be corrected in the proposed EC8-3 revision of 2022. The Greek CSI 2013 adopts a very simple straight-forward analytical procedure producing the most conservative results, while the revised analytical expressions included in the 2022 version, has a better convergence with the experiments. However, for large thickness of confinement material, the ductility factor values are unrealistically high. The model proposed in the literature has the advantage of correcting the aforementioned unrealistic result.

Keywords

FRP sheet reinforcement, ductility enhancement, RC columns

1 Introduction

In all seismic prone countries, codes and standards for the seismic design and assessment of structures provide rules for safety. However, the recent catastrophic earthquakes in Turkey have tragically proven once again the importance of the seismic design and accurate implementation of this design on structures. In many cases of severely damaged buildings, the lack of ductility, particularly in primary seismic columns, was found out to be a very crucial parameter that leads failure to develop into total/fatal collapse. Therefore, the enhancement of ductility in columns could serve also as a strengthening and/or retrofitting strategy to improve the seismic behaviour of existing RC buildings, protecting the lives of its residents [1].

Among other methods and techniques, increasing ductility can be achieved through confinement with composite fibre reinforced polymers (FRPs). In the literature, there are various analytical procedures proposed to determine the increase of ductility. The current paper is a continuation of previous research works [1],[2] that proposes a further analytical formulation for calculating the ductility factor after the confinement of RC columns with FRP sheets. In addition to the proposed analytical relationship, the comparison includes respective equations that are proposed in the previous and in the current draft version of Eurocode 8-part 3 (EC8-3), along with similar equations proposed in the previous and the revised version of the Greek Code for Structural Interventions.

The results deriving from the available analytical formulations, as well as a further proposed analytical relationship are compared with experimental results, and then factors affecting the strengthening efficiency, such as the thickness of the confining material and the reduced axial load, are further investigated and discussed.

2 Available analytical procedures to determine local ductility

Ductility of a member is its ability to deform beyond its yield point, i.e., to develop permanent deformations, without a significant reduction of its maximum strength. In other words, ductility of structures could keep their integrity, although severe or significant damages can occur. In the current paper, the analytical procedures that concern the evaluation of ductility in the Eurocode 8 and the Greek code for structural interventions are investigated. More specifically, in sections 2.1 to 2.5 the following codes are considered: (a) Eurocode 8-Part 3 (2005) [3], (b) Draft of Eurocode 8-Part 3 in conjunction with Part 1 (2022) [4],

© 2023 The Authors. Published by Ernst & Sohn GmbH.

https://doi.org/10.1002/cepa.2174

This is an open access article under the terms of the Creative Commons Attribution-NonCommercial-NoDerivs License, which permits use and distribution in any medium, provided the original work is properly cited, the use is non-commercial and no modifications or adaptations are made.

(c) Greek CSI (2013) [5] and (d) the 2nd revision of the Greek CSI (2022) [6], together with an analytical model proposed by the second and third author of the present work (2019) [7].

2.1 Eurocode 8 – Part 3 (EC8-3) (2005) [3]

The ductility factor μ_θ is defined as the ratio: $\mu_\theta=\theta_u/\theta_y$. The value of the chord rotation at yield (θ_y) is assumed to be unaffected by the confinement and is calculated as for the unconfined elements from the relation:

$$\theta_y = \frac{\varphi_y(L_v+\alpha_v z)}{3} + 0.0014(1+1.5h/L_v) + \frac{\varphi_y d_{bL} f_y}{8\sqrt{f_c}} \quad (1)$$

Where, φ_y is the curvature at yield, L_v is the shear length of the member, $a_v z$ is the tension shift of the bending moment diagram, h is the height of the section, d_{bL} is the mean diameter of the tensile reinforcement, f_y and f_c is the mean yield strength of the steel reinforcement bars and the mean compressive strength of the concrete, respectively.

The value of the chord rotation at failure θ_u is determined through two semi-empirical relationships. Either from the relationship below [3]:

$$\theta_u = 0.016(0.3^\nu)\left[\frac{\max(0.01;\omega')}{\max(0.01;\omega_{tot}-\omega')} f_c\right]^{0.225}\left(\frac{L_v}{h}\right)^{0.35} 25^{\left(a\rho_{sx}\frac{f_{yw}}{f_c}+a_f\rho_f\frac{f_{f,e}}{f_c}\right)}(1.25^{100\rho_d}) \quad (2)$$

Or through the relationship $\theta_u = \theta_y + \theta_u^{pl}$, where θ_u^{pl} is calculated from the following relationship:

$$\theta_u^{pl} = 0.0145(0.25^\nu)\left[\frac{\max(0.01;\omega')}{\max(0.01;\omega_{tot}-\omega')} f_c\right]^{0.3}\left(\frac{L_v}{h}\right)^{0.35} 25^{\left(a\rho_{sx}\frac{f_{yw}}{f_c}+a_f\rho_f\frac{f_{f,e}}{f_c}\right)}(1.275^{100\rho_d}) \quad (3)$$

Where, ν is the normalised axial load referring to ($b\cdot h$), ω_{tot} and ω' is the mechanical ratio of the total and compressive reinforcement, respectively, ρ_{sx} and ρ_d is the geometric ratio of the transverse reinforcement in the direction of loading and of any bidiagonal reinforcement, respectively, a is the confinement effectiveness factor of the stirrups and f_{yw} is the yield strength of the stirrups, $\rho_f = 2t_f/b$ is the geometric ratio of the FRP in the direction of loading, t_f is the thickness of the FRP. a_f is the confinement effectiveness factor of the FRP. Considering the beneficial effect of rounding the corners of the sections by radius R, a_f, is estimated by the following expression:

$$a_f = 1 - \frac{(b-2R)^2+(h-2R)^2}{3bh} \quad (4)$$

where b is the width of cross section, ρ_f and t_f as defined above and $f_{f,e}$ is the effective stress of FRP given by:

$$f_{f,e} = f_{ue}\left(1 - 0.7 f_{ue}\frac{\rho_f}{f_c}\right) \quad (5)$$

where $f_{ue}=min\ (f_u;\ \varepsilon_{u,f}\ E_f)$ with f_u and E_f are the strength and the modulus of elasticity of the FRP, respectively. $\varepsilon_{u,f}$ is the ultimate strain of the FRP and is taken as 0,015 for carbon FRP (CFRP) or 0,02 for glass FRP (GFRP).

2.2 Draft of Eurocode 8 – Part 3 (2022) [4]

In the draft of EC8-3 (2022), the previous relationship (1) that determines θ_y is modified with respect to the middle factor and takes the form:

$$\theta_y = \frac{\varphi_y(L_v+\alpha_1)}{3} + 0.0019(1+h/(1.6L_v)) + \frac{\varphi_y d_{bL} f_y}{8\sqrt{f_c}} \quad (6)$$

φ_y is the yield curvature that can be calculated from a section analysis and a_1 is the tension shift of the bending moment diagram according to PrEN 1992-1-1:2021, which should be taken equal to zero in rectangular columns with clear height-to-depth ratio above 6.5.

The chord rotation at failure θ_u is calculated in two alternative ways. The first through the relationship $\theta_u=\theta_y+\theta_u^{pl}$, where θ_u^{pl} is determined by the semi-empirical relation:

$$\theta_u^{pl} = \kappa_{axial}\cdot\kappa_{reinf}\cdot\kappa_{concrete}\cdot\kappa_{shearspan}\cdot\kappa_{confinement}\cdot\theta_{u0}^{pl} \quad (7)$$

$$\kappa_{axial} = 0.2^\nu \quad (8)$$

$$\kappa_{reinf} = \left[\frac{max(0.01,\omega')}{max(0.01,\omega_{tot}-\omega')}\right]^{0.25} \quad (9)$$

$$\kappa_{concrete} = \left[min\left(2,\frac{f_c(MPa)}{25}\right)\right]^{0.10} \quad (10)$$

$$\kappa_{shearspan} = \left[\frac{1}{2.5}\min\left(9,\frac{L_v}{h}\right)\right]^{0.35} \quad (11)$$

$$\kappa_{confinement} = 24^{max\left[\left(\frac{\alpha\rho_{sx}f_{yw}}{f_c}\right),\left(\frac{\alpha\rho f_u}{f_c}\right)_f\right]} \quad (12)$$

With $\left(\frac{\alpha\rho f_u}{f_c}\right)_f = \alpha_f\cdot c_f\cdot\lambda(1-0.5\lambda)$ (13)

and $\lambda = min\left(0.4,\ \ k_{eff}\cdot\varepsilon_{u,f}\cdot E_f\cdot\rho_f/f_c\right)$ (14)

c_f =1.9 for CFRP, c_f =1.15 for GFRP.

For structural elements with rectangular cross-sections, it is concerned $\theta_{u0}^{pl} = 0.039$.

Also, k_{eff} is the FRP effectiveness factor equal to 0.6, E_f is the elastic modulus of FRP and $\varepsilon_{u,f}$ is the ultimate strain of the FRP, which may be taken equal to 0.015 for CFRP and 0.02 for GFRP.

The second alternative way of determining θ_u is through the general theoretical expression of [4]:

$$\theta_{um} = \theta_y + (\varphi_u-\varphi_y)L_{pl}(1-0.5L_{pl}/L_v) + \Delta\theta_{u,slip} \quad (15)$$

$\Delta\theta_{u,slip}$ is the post-yield fixed-end rotation due to yield penetration in the anchorage zone beyond the yielding end of the member, taken as:

$$\Delta\theta_{u,slip}=9.5d_{bL}(\varphi_u+\varphi_y)/2 \quad (16)$$

L_{pl} is the plastic hinge length of the member. The curvatures φ_y and φ_u are determined, considering the mechanical characteristics of the confined concrete, as it is described in this code in detail, taking into account, if the ultimate strains occur before or after spalling of the concrete cover.

2.3 Greek CSI (2013) [5]

The ductility factor in terms of rotations μ_θ is determined through the ductility factor in terms of curvatures μ_φ from the approximate relationship:

$$\mu_\theta = (\mu_\varphi + 2)/3 \quad (17)$$

With $\mu_\varphi = \frac{\varepsilon_{cu,c}}{2.2 \cdot \nu \cdot \varepsilon_{sy}} \quad for\ \nu \geq 0.2$ (18)

Where $\varepsilon_{cu,c}$ is the ultimate strain of the confined concrete and ε_{sy} is the yield strain of the longitudinal reinforcement.

The strain of confined concrete at failure is calculated as follows:

$$\varepsilon_{cu,c} = \gamma_{FRP} \cdot 0.0035(f_{cc}/f_c)^2 \quad (19)$$

Where γ_{FRP}=1 for CFRP and γ_{FRP}=2 for GFRP and f_{cc} is the strength of the confined concrete that is given by the following equation:

$$f_{cc} = (1.125 + 1.25 a_f \omega_{wd}) f_c \quad (20)$$

With $a_f \omega_{wd} = a_f \rho_{fw} f_{fu}/f_c$ being the efficient confinement ratio, α_f is as defined in section 2.1 and $\rho_{fw} = 2 \cdot min\left(\frac{2t_f}{h}, \frac{2t_f}{b}\right)$ and $f_{fu} = f_{fu,res} \cdot \psi$ is the effective reduced value of the confining strength, where $f_{fu,res}$ is calculated based on the "residual" strain at failure of the added material $\varepsilon_{fu,res} = \varepsilon_u - \varepsilon_o$, ε_u is the strain at failure of the FRP and $\varepsilon_o = t_1/2R$ is the local reduction of the available strain at failure (t_1 is the thickness of one layer) due to bending of the FRP at the corners of the structural element and $\psi = k^{-1/4} \geq 3/k$ is the influence coefficient of the number of layers (k) for k≥4.

2.4 Greek CSI (2022) [6]

In the revised version of the Greek CSI in 2022, all previous equations still apply, except for Eq. (18) that is modified as follows:

$$\mu_\varphi = \frac{f_{cc}}{f_c} \frac{\varepsilon_{cu,c}}{2.6 \cdot \nu \cdot \varepsilon_{sy}} \quad (21)$$

and the confined concrete strength is estimated by the expression:

$$f_{cc} = \left(1 + 3{,}5\left(\frac{\alpha_f \rho_f f_{fu}}{f_c}\right)^{\frac{3}{4}}\right) f_c \quad (22)$$

where $\rho_f = 2t_f/b$, α_f is as defined in section 2.1 and f_{fu} is estimated as defined in section 2.3.

2.5 Analytical Model of [7]

The analytical formulation proposed in the following Eq. (23) lies in a similar concept to Eq. (21) of the Greek CSI 2022 above, and a detailed documentation can be found in [7].

$$\mu_\varphi = \min\left(\frac{f_{cc}}{f_c} \frac{\varepsilon_{cu,c}}{2.3\nu \cdot \varepsilon_{sy}}, \frac{\varepsilon_{su} + \varepsilon_{cu,c}/3}{(1 - \nu f_c/f_{cc}) 1.52 \varepsilon_y}\right) \quad (23)$$

All the parameters of Eq. (23) are as defined in section 2.4. The main difference among these equations is that Eq. (21) considers only the possibility of failure of the cross-section through breaking of the extreme compressive concrete fibre of the cross-section. Eq. (23) apart from that also considers the possibility of failure of the tensile reinforcement.

3 Comparison of analytical models with experimental results

In this section, the analytical results deriving from the above presented models are compared with experimental results on FRP-confined columns, acquired from tests that have been conducted at the Department of Civil Engineering of the University of Patras, Greece [8], [9], [10], [11].

3.1 Experimental results

The experimental data selected for the comparison are presented in Table 1. More specifically, in Table 1 for each specimen, its geometrical and material properties are documented. Cross sections S, W and R are rectangular, while Qs, Ls and L are quadratic. In the notation of each specimen, the second letter symbolizes the material of the confinement reinforcement (C for carbon and G for glass), while the number represents the number of FRP layers.

All the examined elements have a shear length of 1.6m and are reinforced with stirrups of 8 mm diameter at spacing of 200mm. CFRP and GFRP sheets are used for external confinement. Specimens denoted by S, W, R and Q_s are confined with CFRPs that have material properties of E_f=230GPa, f_u=3450MPa, t_1=0.13mm and R=30mm. Specimens L_s and L are CFRP confined with E_f=225GPa, f_u=3800MPa, t_1=0.17mm and R=25mm. While further S and W specimens are also confined with GFRP with E_f=70GPa, f_u=2170MPa, t_1=0.17mm and R=30mm.

From the experimental results, the force-displacement hysteresis loops are available, through which the ductility factor μ_θ is obtained. In Figure 1, a typical M-θ curve is depicted and through these curves the values of θ_y and θ_u were derived.

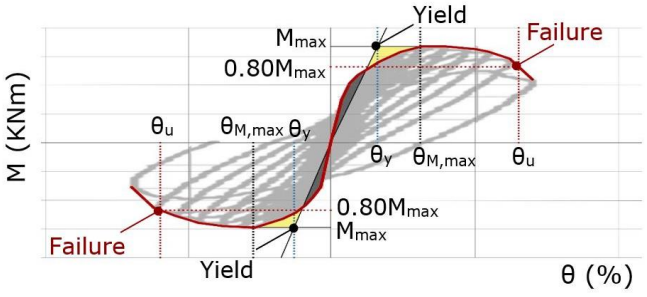

Figure 1 Typical M-θ curve of the experimental results

The values θ_y and θ_u are obtained from the average of the corresponding positive and negative values. Then the ductility factor values μ_θ for each specimen is obtained as $\mu_\theta = \theta_u/\theta_y$.

Table 1 Cross-sectional data from experiments

Specimen		v	f_c (MPa)	d (mm)	b (mm)	h (mm)	n/d_{bL} (mm)	f_y (MPa)	f_t (MPa)	f_{yw} (MPa)
S_C2	[8]	037	18.1	470	250	500	4Ø18	559.5	682	286
S_C5	[8]	0.39	17.9	470	250	500	4Ø18	559.5	682	286
S_G5	[8]	0.37	18.7	470	250	500	4Ø18	559.5	682	286
W_C2	[8]	0.37	18.1	218	500	250	4Ø18	559.5	682	286
W_C5	[8]	0.39	17.9	218	500	250	4Ø18	559.5	682	286
W_G5	[8]	0.37	18.7	218	500	250	4Ø18	559.5	682	286
R_C2	[9]	0.23	32.9	462	250	500	4Ø18	514	659	425
R_C5	[9]	0.23	32.9	460	250	500	4Ø18	541	659	425
Q_s_C2	[10]	0.45	28.1	215	250	250	4Ø14	313	442	425
Q_s_C5	[10]	0.44	28.2	215	250	250	4Ø14	313	442	425
L_s_C2	[11]	0.28	30.3	210	250	250	4Ø14	372	433	351
L_C2	[11]	0.28	28.9	225	250	250	4Ø14	523	624	351

3.2 Results comparison in terms of ductility

The analytical models are implemented for each individual specimen with the properties described in Table 1. The analytical model of [7] is implemented in two ways. The first is applied, considering the multiple layers reducing coefficient ψ, as defined in the Greek CSI 2022 (see section 2.3) (Proposal a), while in the second, ψ is not considered (Proposal b).

Table 2 presents the ductility factor μ_θ values of the experiments in the second column, while in the rest of the table the ratios of the analytical (μ_θ^{ANAL}) to the experimental (μ_θ^{EXP}) ductility factors are presented. As it can be noted from Table 2, Greek CSI 2013 produces for all cases the most conservative values, while Greek CSI 2022 gives a deviation of the mean value of 18% in favour of safety and seems to have a much better convergence with the experiments, however with a coefficient of variation of 43%. The results of the analytical model of [7] are less conservative than those of Greek CSI 2022 with the same coefficient of variation, while proposal (b) seems to converge on average better than (a). However, some values resulting from proposal (b) significantly exceed the experimental ones, something that does not result from proposal (a).

The results from Eq. (2) and Eq. (1) +(3) of EC8-3 (2005), as well as Eq. (6) + (7) of the EC8-3 (2022) draft, have good convergence with the experiments (see Table 2). The EC8-3 (2005) relations show a coefficient of variation of 27%, while the respective value for Eq. (6) + (7) is 34%. Eq. (15) of the EC8-3 (2022) draft produces very conservative values with an average deviation of 41% (see Table 2).

4 Influence of the number of FRP layers

To further investigate the influence of the FRP thickness and the respective number of layers, a series of comparative figures for all analytical models is created. In the current paper, indicatively, the results on the specimens with rectangular cross-sections S and R and with the square cross-section Q_s are presented.

Figures 2 and 3 show the change in the ductility factor μ_θ, as obtained from each analytical model, as a function of the number of the FRP layers, for cross-sections S and R, respectively. Figures 4 and 5 show the variation of μ_θ for cross section Q_s as a function of the FRP thickness and number of layers, respectively.

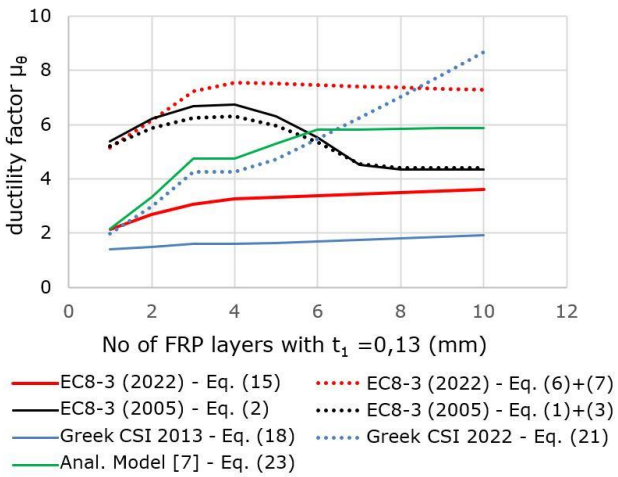

Figure 2 Ductility factor as a function of the layers k of the FRP - S Section with v=0.38

Table 2 Values of $\mu_\theta^{EXP.}$ and $\mu_\theta^{ANAL.}$ / $\mu_\theta^{EXP.}$

Cross-section	$\mu_\theta^{EXP.}$ (%)	Greek CSI		Eq. (23) from [7]		EC8-3 (2005)		Draft EC8-3 (2022)	
		2013 Eq. (18)	2022 Eq. (21)	Proposal (a)	Proposal (b)	Eq. (2)	Eq.(1) + Eq.(3)	Eq.(6) + Eq.(7)	Eq. (15)
S_C2	4.00	0.38	0.76	0,85	0,85	1,56	1,48	1,54	0,68
S_C5	4.68	0.35	0.99	1,11	1,25	1,36	1,28	1,60	0,70
S_G5	6.14	0.42	1.22	1,02	1,04	1,07	1,00	0,90	0,48
W_C2	5.46	0.28	0.37	0,40	0,40	0,76	0,78	0,77	0,41
W_C5	5.73	0.28	0.45	0,50	0,69	0,89	0,87	0,94	0,50
W_G5	6.04	0.42	0.69	0,77	1,03	0,72	0,73	0,66	0,39
R_C2	5.92	0.34	0.54	0,59	0,59	0,99	0,96	0,94	0,45
R_C5	7.33	0.29	0.62	0,69	0,79	0,97	0,91	1,02	0,52
Qs_C2	6.60	0.34	0.64	0,72	0,72	0,86	0,81	0,74	0,44
Qs_C5	6.66	0.41	0.94	1,06	1,46	1,07	0,97	1,07	0,67
Ls_C2	5.74	0.52	1.10	1,23	1,23	1,04	1,00	1,05	0,74
L_C2	3.11	0.77	1.58	1,77	1,77	1,61	1,60	1,66	1,10
Mean Value		**0.40**	**0.82**	**0.89**	**0.99**	**1.07**	**1.03**	**1.07**	**0.59**
Variation Coefficient (%)		**34**	**43**	**42**	**40**	**27**	**27**	**32**	**34**

In all Figures 2 to 5, it can be concluded that μ_θ from Eq. (2) (black solid line) and Eq. (1)+(3) (black dotted line) of EC8-3 (2005), which are in good agreement with each other, appear to increase up to a limit value corresponding to a certain material thickness or number of layers. After this maximum value that lies between 4 and 6 FRP layers in these examples, the values start decreasing, a fact which is not logical and is observed more strongly in Figure 2. In terms of thickness, the maximum limit value, derives from the equation $t_{f,lim} = f_c b/0.042E_f$.

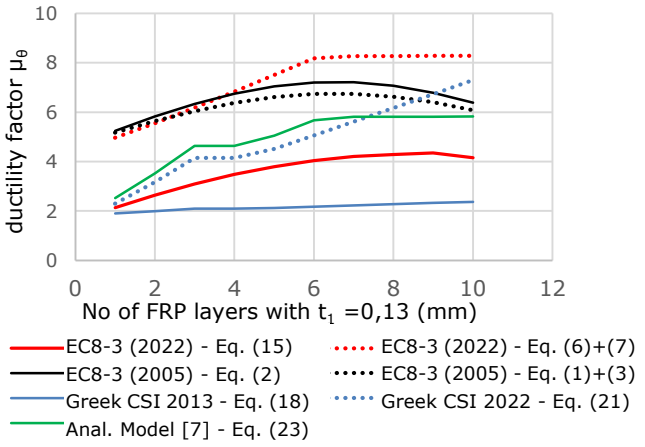

Figure 3 Ductility factor as a function of the layers k of the FRP - R Section with v=0.23

The paradox decrease in μ_θ as the confinement material increases, observed above, is corrected in Eq. (6)+(7) (red dotted line) of the draft EC8-3 (2022), as a limit is applied to the confinement efficiency, resulting to a constant ductility factor value after a certain thickness of FRP material is applied. Through Eq. (6)+(7), this limit is determined as follows:

$$t_{f,lim} = f_c b/3\varepsilon_{u,f} E_f \quad (24)$$

where for CFRP it becomes $t_{f,lim} = f_c b/0.045E_f$.

Regarding the ductility values of Eq. (15) (red solid line) of the EC8-3 (2022) draft, they appear to be considerably more conservative.

From Eq. (18) of the Greek CSI 2013 (blue solid line), the results appear to be the most conservative, as it was also previously realised in Table 2, and the increase in the number of FRP layers or in the thickness doesn't seem to influence the ductility factor. On the other hand, in the values resulting from Eq. (21) of the Greek CSI 2022 (blue dotted line), there is a continuous increase of the ductility factor in relation to the layers of the confinement material, almost in a linear manner, as it can be clearly seen in Fig 4.

The proposed analytical model of [7] (green solid line) produces similar results to those of the Greek CSI 2022, however, the excessively high values of μ_θ (compared to EC8-

3), which resulted from the Eq. (21) of the Greek CSI 2022, for multiple FRP layers, are corrected, reaching also a constant value of the ductility factor after a certain thickness or number of layers of the FRP.

In Figures 4 and 5, it can also be noted that the analytical formulations of both EC8-3 versions result to the same μ_θ values, regardless of whether they are applied as a function of the thickness t_f, or as a function of the number of layers k. On the contrary, in the analytical formulations of the Greek CSI for k≥3 a significant variation is observed, with μ_θ values being very high when calculated as a function of thickness. This fact is more strongly observed in Greek CSI 2022. This differentiation of the results for k≥3 is also present in the proposed analytical model of [7], but to an apparently much smaller extent.

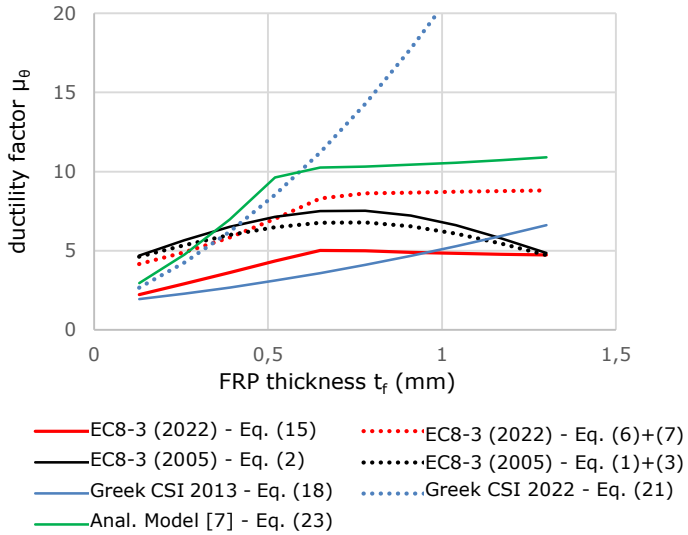

Figure 4 Ductility factor as a function of the FRP thickness- Q_s Section with v=0.25

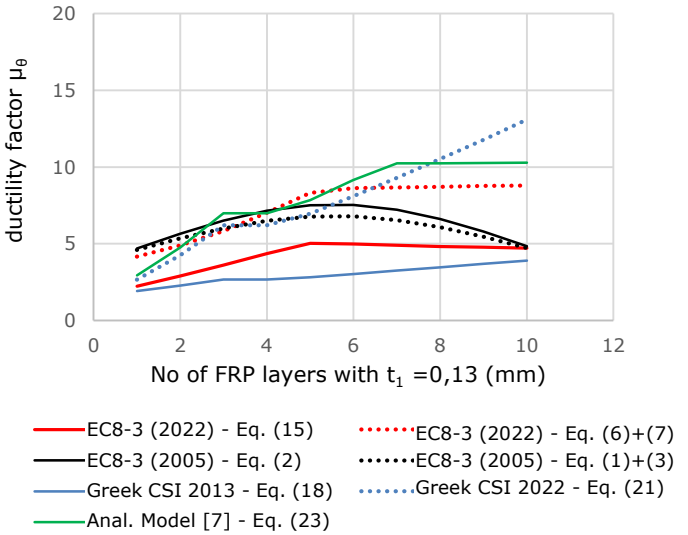

Figure 5 Ductility factor as a function of the layers k of the FRP - Q_s Section with v=0.25

5 Conclusions

In the present work, a series of analytical models from the literature for the determination of the ductility factor are presented and compared with each other and with relevant experimental results. The main conclusions from this comparison are the following:

- The analytical models of the Greek CSI 2013 lead on average to the most conservative ductility values in all cases, in comparison with the other models, while the 2022 version has a much better convergence with the experiments. At the same time, the 2022 version results in more conservative values compared to the respective ones from the semi-empirical relationships of EC8-3 (2005) and EC8-3 draft (2022).

- The results according to [7] have better convergence compared to the Greek CSI 2022, particularly in proposal (b), when the multiple layers reducing coefficient ψ is ignored. In this case, the mean value was found to be almost the same as in the experimental results.

- The ductility values obtained through the semi-empirical relations given in Eq. (2) and Eq. (1)+(3) of the EC8-3 (2005) and Eq. (6)+(7) of the EC8-3 (2022) have no substantial differences compared with each other and have fairly good convergence with the experiments. On the contrary, the theoretical relation in Eq. (15) of the EC8-3 (2022) draft is very conservative.

- The results of the Greek CSI 2022 and of [7] show a dispersion of around 40%, while their counterparts of EC8-3 show a smaller dispersion of around 30%.

- In the analytical models of EC8-3 (2005), an unrealistic response occurs after the application of a certain thickness of reinforcement material. As after the application of this limiting thickness the value of the ductility factor appears to decrease. In EC8-3 (2022), the semi-empirical relation of Eq. (6)+(7) produces similar results to those of the aforementioned relations, while at the same time the unrealistic reduction in ductility observed in EC8-3 (2005) is restored, introducing a limit to the confinement efficiency.

- The theoretical relationship of the Eq. (15) of the draft of EC8-3 (2022) produces more conservative results compared to the rest of the models except for the one of Greek CSI 2013.

- In Greek CSI 2022, for large thicknesses of confinement material, the ductility values are unrealistically very high (compared to EC8-3). This anomaly is corrected by the proposed Eq. (23) of the analytical model by [7].

References

[1] Dritsos S. (2005). *Repair and Strengthening of Structures*. University of Patras, Patras (in Greek).

[2] Athanasopoulou S.; Christodoulou M.; Dritsos S. (2016). *Seismic Strengthening of Columns with Deficient Ductility and Capacity*. 19th IABSE Congress Stockholm: *Challenges in Design and Construction of an Innovative and Sustainable Built Environment*, p.p. 1026-1033.

[3] Eurocode 8 *Design of Structures for Earthquake Resistance* - Part 3 *Assessment and Retrofitting of Buildings*, EN 1998-3:2005, European Committee for Standardization.

[4] Eurocode 8. *Design of Structures for Earthquake Resistance. Part 3: Assessment and Retrofitting of Buildings and Bridges*, Draft EN 1998-3:2022-07-14 and Part 1-1: General Rules and Seismic Action, Draft PrEN1998-1-1: Sept. 2022, European Committee for Standardization.

[5] Greek CSI (2013), Greek Earthquake Planning and Protection Organization, Greek Ministry for Environmental Planning and Public Works, Athens, Greece.

[6] Greek CSI (2022), 2nd Revision, Greek Earthquake Planning and Protection Organization, Greek Ministry for Environmental Planning and Public Works, Athens, Greece (in Greek).

[7] Liakopoulou E.; Dritsos S. (2019). *Ductility of RC Columns confined with FRPs*. 4th Greek Conference on Earthquake Engineering and Technical Seismology, Athens (in Greek).

[8] Bousias, S.N.; Triantafillou, T.C.; Fardis, M.N.; Spathis, L.; O'Regan, B.A. (2004). *Fiber reinforced polymer retrofitting of rectangular reinforced concrete columns with or without corrosion*. ACI Structural Journal, 101-S51, pp. 512-520.

[9] Bousias, S.N.; Spathis L.; Fardis, M.N. (2006). *Concrete or FRP jacketing of columns with lap splices for seismic rehabilitation*. Journal of Advanced Concrete Technology *Vol. 4*, No. 3, pp. 1-14.

[10] Bousias, S.N.; Spathis, L.; Fardis M.N. (2007). *Seismic retrofitting of columns with lap spliced smooth bars through FRP or concrete jackets*. Journal of Earthquake Engineering, 11, pp. 653-674.

[11] Bournas, D. A. (2008). *Strengthening of RC columns with novel materials: FRPs, reinforcement of composite materials or stainless steel in notches*. Doctoral Dissertation, University of Patras, Polytechnic School, Department of Civil Engineering, Patras, Greece (in Greek).